

---

# HOMOTOPY-AWARE MULTI-AGENT PATH PLANNING ON PLANE

---

A PREPRINT

**Kazumi Kasaura**  
OMRON SINIC X Corporation  
kazumi.kasaura@sinicx.com

October 30, 2024

## ABSTRACT

We propose an efficient framework using Dynnikov coordinates for homotopy-aware multi-agent path planning in planar domains that may contain obstacles. We developed a method for generating multiple homotopically distinct solutions for the multi-agent path planning problem in planar domains by combining our framework with revised prioritized planning and proved its completeness under specific assumptions. Experimentally, we demonstrated that our method is significantly faster than a method without Dynnikov coordinates. We also confirmed experimentally that homotopy-aware planning contributes to avoiding locally optimal solutions when searching for low-cost trajectories for a swarm of agents in a continuous environment.

## 1 Introduction

In robot planning and navigation, considering topological features of paths is crucial in various aspects. For example, it becomes significant when seeking globally optimal trajectories. While a conventional strategy is to plan an initial path on a simple graph (e.g., grid) and optimize it to minimize cost, it may lead to local optima since optimization does not alter topological characteristics. Since which path is optimized to a globally optimal solution can be hardly known beforehand, it was proposed to generate several topologically distinct paths [Kuderer et al., 2014, Rösmann et al., 2017]. Topological awareness in planning also finds relevance in tasks such as cable manipulation [Bhattacharya et al., 2015, Kim et al., 2014], human-robot interaction [Govindarajan et al., 2016, Yi et al., 2016], and high-level planning with dynamic obstacles [Cao et al., 2019].

*Homotopy* is a straightforward topological feature of paths, but difficult to calculate due to its non-abelian nature. Bhattacharya and Ghrist [2018] proposed an approach on the basis of a concept called the *homotopy-augmented graph* for general homotopy-aware path planning. Homotopy-aware path planning using a roadmap is reduced to pathfinding on the homotopy-augmented graph constructed from the roadmap.<sup>1</sup> To search on a homotopy-augmented graph, we have to manage elements of the *homotopy group* of the searched space. Elements of the group are represented by strings of generators, called *words*. However, different words can represent the same element of the group, and determining the identity of such representations, termed the *word problem*, is not generally solvable [Novikov, 1955]. Consequently, homotopy-aware path planning remains a generally difficult task.

On the other hand, multi-agent path planning, which plans paths for multiple agents so that they do not collide with each other, has a variety of application [Silver, 2005, Dresner and Stone, 2008, Li et al., 2020]. In multi-agent scenarios on a plane, topological features are nontrivial even in the absence of obstacles since agents are obstacles for other agents. For example, when two agents pass each other, the topological characteristics of the solution differ depending on whether they avoid each other counterclockwise or clockwise as shown in Figure 1. Homotopical consideration is important in multi-agent coordination [Mavrogiannis and Knepper, 2019], especially for avoiding deadlocks [Čáp et al., 2016]. However, studies on homotopy-aware planning for multi-agent scenarios, even in obstacle-free environments, are limited.

---

<sup>1</sup>Since we focus on the approach of using roadmaps for path planning, the problem that we treat in this paper is actually pathfinding on graphs. However, the homotopies we consider are not those in discrete graphs [Ghrist, 1999] but those in the continuous domain. Thus, to avoid confusion, we do not use the term *homotopy-aware pathfinding*.

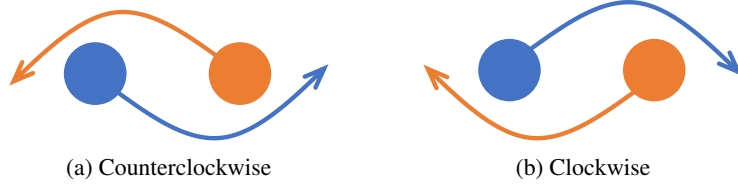


Figure 1: Two ways for two agents to pass each other

By combining the aforementioned concepts with research for braids, we obtained an efficient framework for homotopy-aware multi-agent path planning in planar domains, which is the first valid solution to this problem to our knowledge. There are three key ideas. First, while the fundamental group for the multi-agent path planning problem on a plane is the *pure braid group*, we label the homotopy classes of solutions by elements of the *braid group*. This is equivalent to expanding the solution space to solutions of *unlabeled* multi-agent path planning, in which, as long as each goal is reached by only one agent, it is permissible for any agent to proceed to any goal. [Adler et al., 2015]<sup>2</sup>. This simplifies the word construction. Since homotopy classes inherently contain information about agent-goal correspondences, this idea does not give rise to any confusion. The second idea is to use *Dynnikov coordinates*, a representation of elements of the braid group as tuples of integers, which can be easily calculated. Thanks to these coordinates, we can efficiently maintain a homotopy-augmented graph by using a data structure such as self-balancing binary search trees [Knuth, 1998]. The third is that obstacles in the domain are taken into account by considering them as virtual agents.

By combining this framework with the *revised prioritized planning* [Čáp et al., 2015], we obtained a method for generating multiple homotopically distinct solutions for multi-agent path planning in a planar domain. We also prove that our method can generate solutions belonging to all homotopy classes under certain assumptions.

We experimentally demonstrate that the runtime of our method increases roughly quadratically with respect to the number of agents on a scale of several hundred agents, while the runtime of another method, which uses the Dehornoy order [Dehornoy, 1994] to manage braids instead of Dynnikov coordinates, increases approximately quintically. In addition, to confirm the usefulness of homotopy-awareness in this situation, we experimentally show that optimizing homotopically distinct solutions generated by our method leads to finding low-cost trajectories.

In summary, the contributions of this paper are that it proposes the first sound algorithm for solving homotopy-aware multi-agent path planning and that it experimentally shows that solving this problem contributes to trajectory optimization.

## 2 Related Work

### 2.1 Multi-Agent Path Planning

Multi-agent pathfinding, a field of study focusing on planning for multiple agents in discrete graphs, has been a subject of extensive research, particularly in grid-based environments [Stern et al., 2019]. One of the approaches to this problem is prioritized planning [Erdmann and Lozano-Perez, 1987, Silver, 2005], which is non-optimal, incomplete yet scalable. Čáp et al. [2015] proposed a revised version of prioritized planning and proved its completeness under certain assumptions. Major optimal approaches for multi-agent pathfinding include increasing-cost tree search [Sharon et al., 2013], conflict-based search [Sharon et al., 2015], and some reduction-based methods [Surynek et al., 2016, Barták et al., 2017]. Surveys of solutions have been conducted by Stern [2019] and Lejeune et al. [2021].

For multi-agent path planning in continuous environments, the typical strategy involves a three-step process: roadmap generation, discrete pathfinding, and, if necessary, continuous smoothing of trajectories. For instance, Hönig et al. [2018] presented such an approach for quadrotor swarm navigation. Several roadmap-generation methods tailored for multi-agent scenarios have been proposed [Henkel and Toussaint, 2020, Arias et al., 2021, Okumura et al., 2022]. A number of multi-agent pathfinding algorithms have been adapted to handle continuous time scenarios [Yakovlev and Andreychuk, 2017, Walker et al., 2018, Andreychuk et al., 2022, Surynek, 2019].

<sup>2</sup>This setting is also called *permutation-invariant* [Kloder and Hutchinson, 2006, Yu and LaValle, 2013] or *anonymous* [Stern et al., 2019].

## 2.2 Topology-Aware Path Planning

For homotopy-aware single-agent path planning on a plane with polygonal obstacles, there exist methods using polygon partition [Park et al., 2015, Liu et al., 2023] with analysis of time complexity [Hernandez et al., 2015, Efrat et al., 2006, Bespamyatnikh, 2003]. For scenarios involving possibly non-polygonal obstacles, several approaches have been explored [Jenkins, 1991, Hernandez et al., 2015, Yi et al., 2016, Schmitzberger et al., 2002]. Grigoriev and Slissenko [1997, 1998] proposed a method of constructing words by detecting traversing *cuts*, which are also called *rays* [Tovar et al., 2010]. Along this idea, the notion of the *homotopy-augmented graph* (*h-augmented graph*), was proposed and applied to the navigation of a mobile robot with a cable [Bhattacharya et al., 2015, Kim et al., 2014]. This approach was generalized by Bhattacharya and Ghrist [2018] to various situations including multi-agent path planning on a plane. However, their algorithm is incomplete. While they attempted to solve the word problem by using Dehn’s algorithm [Lyndon et al., 1977], they acknowledged that this algorithm may not always yield accurate results for their presentation.<sup>3</sup>

*Homology* serves as a coarser classification compared with homotopy, whereby two paths belonging to the same homotopy class are also in the same homology class, but the reverse is not always true<sup>4</sup>. While homology is not well-suited for detailed path analysis like homotopy, it possesses the advantage of being computationally easier due to its abelian nature. Algorithms have been developed for homology-aware path planning in two, three, or higher dimensional Euclidean spaces with obstacles [Bhattacharya, 2010, Bhattacharya et al., 2011, 2012, 2013]. In the planar scenario, homology can be determined by winding numbers [Vernaza et al., 2012] and this knowledge has been applied to enable homology-aware planning for mobile robot navigation [Kuderer et al., 2014]. The winding number is also used for navigation when other agents are present [Mavrogiannis and Knepper, 2020].

## 2.3 Braids and their Applications to Robotics

The braid group was introduced by Artin [1947a,b]. There are several algorithms for solving the word problem of braid groups [Garside, 1969, Epstein, 1992, Birman et al., 1998, Hamidi-Tehrani, 2000, Garber et al., 2002]. Dehornoy [1994] introduced a linear order of braids called the *Dehornoy order*, for which comparison algorithms were presented [Dehornoy, 1997, Maljutin, 2004]. Dehornoy et al. [2008] conducted a survey of orders of braids and their comparison algorithms. It was proved that the braid groups are linear [Bigelow, 2001, Krammer, 2002]. Dynnikov coordinates were introduced by Dynnikov [2002].

In robotics, the concept of braid groups on graphs is used for robot planning on graphs [Ghrist, 1999, Kurlin, 2012]. Regarding the planar case, Diaz-Mercado and Egerstedt [2017] developed a framework enabling the control of agents such that their trajectories correspond to specific braids. In their setting, agents move in circular paths on a predefined track, while our approach deals with path planning with arbitrary start and goal positions.

It was proposed to impose homotopy constraints when executing plans to prevent deadlock even if there are delays [Gregoire et al., 2013, Čáp et al., 2016]. Homotopy constraints were also proposed for use in game-theoretic motion planning in urban driving [Khayyat et al., 2024]. Braid groups were used for predicting trajectories of other agents [Mavrogiannis and Knepper, 2019]. This framework was applied to intersection management [Mavrogiannis et al., 2022].

Lin and McCann [2021] used braids to represent states of a knitting machine to find its optimal plans. While their aim is quite different from ours, their proposed method is similar to ours since it searches for optimal transfer plans for states represented by braids. While they used symmetric normal forms [Dehornoy, 2008] to manage braids, we do not for the reason of computational efficiency.

## 3 Preliminary

### 3.1 Homotopy and Fundamental Group

Let  $X$  be a topological space. A continuous morphism from the interval  $[0, 1]$  to  $X$  is called a *path*. For two paths  $\gamma_0, \gamma_1$  such that  $\gamma_0(1) = \gamma_1(0)$ , we define the composition  $\gamma_0 \circ \gamma_1$  as

$$\gamma_0 \circ \gamma_1(t) = \begin{cases} \gamma_0(2t) & 0 \leq t \leq 1/2, \\ \gamma_1(2t - 1) & 1/2 \leq t \leq 1. \end{cases} \quad (1)$$

<sup>3</sup>Actually, their algorithm fails to perform correctly when dealing with scenarios involving more than three agents (see Appendix A for details).

<sup>4</sup>In the context of robotics, homotopy and homology are sometimes used interchangeably.[Bhattacharya et al., 2012]

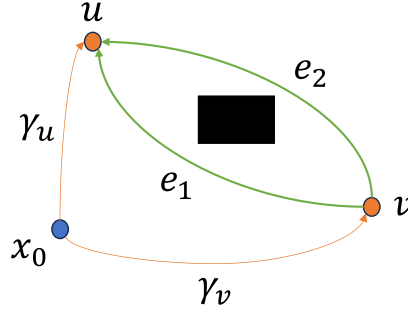


Figure 2: Example of edges with different homotopic traits

Two paths  $\gamma_0$  and  $\gamma_1$  with the same endpoints are said to be *homotopic* if there exists a continuous map  $h : [0, 1] \times [0, 1] \rightarrow X$  such that

$$h(s, 0) = \gamma_0(0) = \gamma_1(0), h(s, 1) = \gamma_0(1) = \gamma_1(1) \quad (2)$$

$$h(0, t) = \gamma_0(t), h(1, t) = \gamma_1(t), \quad (3)$$

for any  $s, t \in [0, 1]$ . The equivalence class of paths under the homotopic relation is called a *homotopy class*. The homotopy class of a path  $\gamma$  is denoted as  $[\gamma]$ .

Consider a point,  $x_0 \in X$ . The set of homotopy classes of closed loops with endpoints at  $x_0$  (i.e.,  $\gamma : [0, 1] \rightarrow X$  such that  $\gamma(0) = \gamma(1) = x_0$ ) forms a group under path composition. The identity element of this group is the homotopy class of the constant map to  $x_0$ . The inverse element of  $[\gamma]$  is  $[\gamma^{-1}]$ , where  $\gamma^{-1}$  is the path following  $\gamma$  in reverse. When  $X$  is path-connected, this group is independent of the choice of  $x_0$  up to isomorphism and denoted as  $\pi_1(X)$ . It is called the *fundamental group of  $X$*  [Hatcher, 2002].

Note that, when  $X$  is path-connected, for any two points  $x_0, x_1 \in X$ , there exists a bijection between homotopy classes of paths from  $x_0$  to  $x_1$  and the fundamental group.

### 3.2 Homotopy-Augmented Graph

Homotopy-aware search-based path planning is reduced to pathfinding on a *homotopy-augmented graph* [Bhattacharya and Ghrist, 2018]. Let  $X$  be a path-connected space, and let  $G = (V, E)$  be a discrete graph (roadmap) on  $X$ . The homotopy-augmented graph  $G_h = (V_h, E_h)$ , which can be considered as a lift of  $G$  into the *universal covering space* of  $X$ , is constructed as follows<sup>5</sup>. We fix a base point  $x_0 \in X$  for the fundamental group. We also assume that one homotopy class  $[\gamma_v]$  of paths from  $x_0$  to each vertex  $v \in V$  is fixed. The construction of  $G_h$  is then expressed as follows:

- $V_h := V \times \pi_1(X)$ , where  $\pi_1(X)$  is the fundamental group of  $X$  with respect to the chosen base point  $x_0$ .
- For each edge  $e \in E$  from vertex  $v \in V$  to vertex  $u \in V$ , and for each element  $\alpha \in \pi_1(X)$ ,  $E_h$  contains an edge from  $(v, \alpha)$  to  $(u, \alpha h(e))$ , where  $h(e) := [\gamma_v \circ e \circ \gamma_u^{-1}]$ . Here,  $\gamma_u$  and  $\gamma_v$  are paths in homotopy classes  $[\gamma_u]$  and  $[\gamma_v]$ , respectively.

Figure 2 is an example. While  $\gamma_v \circ e_1 \circ \gamma_u^{-1}$  is homotopic with the constant function,  $\gamma_v \circ e_2 \circ \gamma_u^{-1}$  is not due to the existence of the obstacle. Thus,  $h(e_1)$  is the unit, and  $h(e_2)$  is the element corresponding to one counterclockwise turn around the obstacle. In the homotopy-augmented graph, two edges above  $e_1$  and  $e_2$  with the same source have different targets.

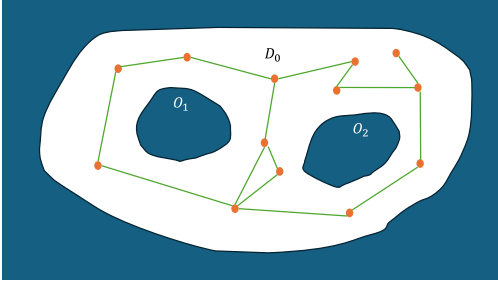
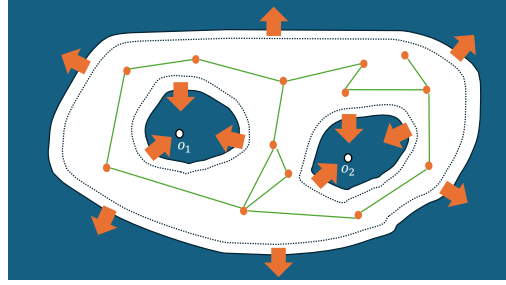
### 3.3 Presentation of Group

A *presentation*  $\langle S|R \rangle$  of a group  $G$  consists of a set  $S \subseteq G$  of generators and a set  $R$  of relations.

In the context of group theory, a *word* is a string consisting of generators and their inverses, which represents an element of the group. *Relations* are words that are considered equal to the identity element in the group.

$\langle S|R \rangle$  satisfies the following conditions.

<sup>5</sup>Our description is generalized from that in the original paper to be independent of how homotopy is calculated.

Figure 3: Example of  $\mathcal{D}$ Figure 4: Deformation of  $\mathcal{D}$ 

- Any element of  $G$  can be represented by a word formed from the generators in  $S$  and their inverses.
- The kernel of the natural surjection from the free group  $F_S$  on  $S$  to  $G$  is the smallest normal subgroup of  $F_S$  containing  $R$ .

A relation  $ab^{-1} \in R$  is sometimes denoted as  $a = b$ .

The decision problem of determining whether two given words represent the same element of the group is known as the *word problem* [Peifer, 1997].

### 3.4 Braid Group

For a domain  $\mathcal{D}$ , the *configuration space*  $\mathcal{C}_n(\mathcal{D})$  is defined as

$$\mathcal{C}_n(\mathcal{D}) := \{(p_1, p_2, \dots, p_n) \in \mathcal{D}^n \mid p_i \neq p_j \text{ for all } i \neq j\}. \quad (4)$$

The  $n$ -th symmetric group  $S_n$  naturally acts on  $\mathcal{C}_n(\mathcal{D})$  by permuting the indices. In the context of unlabeled multi-agent path planning, where we ignore the indices of agents, we consider the *unlabeled configuration space*  $\mathcal{UC}_n(\mathcal{D})$ , which is defined as the quotient of  $\mathcal{C}_n(\mathcal{D})$  by  $S_n$ .

The fundamental group of  $\mathcal{UC}_n(\mathbb{R}^2)$  is known as the  $n$ -th *braid group*  $B_n$ . The fundamental group of  $\mathcal{C}_n(\mathbb{R}^2)$ , which is a subgroup of  $B_n$ , is known as the  $n$ -th *pure braid group*  $P_n$ . There exists a natural surjective group homomorphism from  $B_n$  to  $S_n$ , the kernel of which is  $P_n$ .

$B_n$  has a presentation given by

$$\langle \sigma_1, \dots, \sigma_{n-1} \mid \sigma_i \sigma_j \sigma_i^{-1} \sigma_j^{-1}, \sigma_i \sigma_{i+1} \sigma_i^{-1} \sigma_{i+1}^{-1} \sigma_i^{-1} \sigma_{i+1}^{-1} \rangle, \quad (5)$$

where  $1 \leq i < n - 1$ , and  $i + 1 < j \leq n - 1$  [Rolfsen, 2010].

## 4 Method

In § 4.1, we describe the setting for homotopy-aware path planning in planar domains. In the following four subsections, we describe the framework for calculating homotopy classes. In § 4.6, we provide the algorithm using this framework to generate multiple solutions with different homotopies. In § 4.7, we prove the completeness of this algorithm under specific assumptions.

### 4.1 Problem Setting

We consider homotopy-aware multi-agent path planning with  $n$  agents in the domain  $\mathcal{D} \subseteq \mathbb{R}^2$ . As illustrated in Figure 3, we assume that  $\mathcal{D}$  has the form  $D_0 \setminus (O_1 \cup \dots \cup O_r)$ , where  $D_0$  and  $O_1, \dots, O_r$  (obstacles) are bounded domains whose boundaries are simple closed curves and  $\mathbb{R}^2 \setminus D_0, O_1, \dots, O_r$  neither intersect nor touch.<sup>6</sup>

We assume that a finite graph  $G = (V, E)$  lying on the interior of  $\mathcal{D}$  is given as a roadmap. When starts  $s_1, \dots, s_n \in V$  and goals  $g_1, \dots, g_n \in V$  are given, we want to find multiple solutions for the multi-agent pathfinding problem on  $G$  belonging to different homotopy classes as paths of the configuration space  $\mathcal{C}_n(\mathcal{D})$ , which means that agents are treated as points while homotopy classes are considered. Note that this simplification affects only the computation of homotopy, and sizes of agents can be considered in pathfinding.

<sup>6</sup>Strictly speaking, for example, a domain in a grid with obstacles touching at corners does not satisfy this assumption. However, such obstacles can be considered as one obstacle by widening them slightly at the corners.

*Remark 1.* Ignoring the sizes of agents does not matter in cases with no obstacles because the agents can be far enough apart from each other when deforming paths to other ones. On the other hand, when there exist obstacles, two paths that are actually homotopically distinct when both sizes of agents and obstacles are taken into account may be considered as homotopic. See also § 6. However, the fact that that our homotopical classification is not complete does not mean that it is useless in such cases.

## 4.2 Reduction to Obstacle-Free Case

We take one representative element  $o_i \in O_i$  for each obstacle. Obviously,  $o_1, \dots, o_r$  are different from each other. By taking sufficiently small neighborhoods of boundaries and transforming them, as illustrated in Figure 4, we can deform  $\mathcal{D}$  to  $\mathbb{R}^2 \setminus \{o_1, \dots, o_r\}$  without changing the roadmap. For a rigorous proof, the Jordan–Schönflies theorem [Thomassen, 1992] can be used. Thus, it is enough to calculate homotopies on  $\mathbb{R}^2 \setminus \{o_1, \dots, o_r\}$ . Note that, since the roadmap is not changed, the found paths are lying on the original  $\mathcal{D}$ .

We reduce the calculation of homotopy in  $\mathcal{C}_n(\mathbb{R}^2 \setminus \{o_1, \dots, o_r\})$  to that in  $\mathcal{C}_{r+n}(\mathbb{R}^2)$ . Intuitively, we consider the obstacles as additional agents staying at the same positions. While it is non-trivial that this reduction preserves homotopy classes because obstacles cannot move when deforming paths, the following proposition guarantees it.

**Proposition 2.** *The map*

$$\pi_1(\mathcal{C}_n(\mathbb{R}^2 \setminus \{o_1, \dots, o_r\})) \rightarrow \pi_1(\mathcal{C}_{r+n}(\mathbb{R}^2)) \quad (6)$$

*induced by the embedding*

$$\begin{array}{ccc} \mathcal{C}_n(\mathbb{R}^2 \setminus \{o_1, \dots, o_r\}) & \hookrightarrow & \mathcal{C}_{r+n}(\mathbb{R}^2) \\ \cup & & \cup \\ (p_1, \dots, p_n) & \mapsto & (o_1, \dots, o_r, p_1, \dots, p_n) \end{array} \quad (7)$$

*is injective.*

*Proof.* The map from  $\mathcal{C}_{r+n}(\mathbb{R}^2)$  to  $\mathcal{C}_r(\mathbb{R}^2)$ , which sends  $(p_1, \dots, p_{r+n})$  to  $(p_1, \dots, p_r)$ , is a fiber bundle [Fadell and Neuwirth, 1962], and the fiber at  $(o_1, \dots, o_r)$  is the image of the above embedding. Thus, the following exact sequence of homotopy groups is induced:

$$\pi_2(\mathcal{C}_r(\mathbb{R}^2)) \rightarrow \pi_1(\mathcal{C}_n(\mathbb{R}^2 \setminus \{o_1, \dots, o_r\})) \rightarrow \pi_1(\mathcal{C}_{r+n}(\mathbb{R}^2)), \quad (8)$$

where  $\pi_2(\mathcal{C}_r(\mathbb{R}^2))$  is the second homotopy group of  $\mathcal{C}_r(\mathbb{R}^2)$  [Hatcher, 2002]. Moreover,  $\pi_2(\mathcal{C}_r(\mathbb{R}^2))$  is trivial [Knudsen, 2018].  $\square$

In the following three subsections, we replace  $r + n$  with  $n$  and consider  $\mathcal{C}_n(\mathbb{R}^2)$  for simplicity.

## 4.3 Reduction to Unlabeled Case

As mentioned earlier, in labeled multi-agent path planning, we can calculate homotopy classes as unlabeled multi-agent path planning. To formalize this reduction, let  $G^n = (V^n, E^n)$  be the  $n$ -times direct product of  $G$  minus collision parts, which is a graph on the configuration space  $\mathcal{C}_n$ . We construct a graph  $(V_h^n, E_h^n)$  as follows instead of using the homotopy-augmented graph for  $\mathcal{C}_n$ .

- $V_h^n := V^n \times \pi_1(\mathcal{UC}_n) = V^n \times B_n$ .
- For each edge  $e \in E^n$  from vertex  $v \in V^n$  to vertex  $u \in V^n$ , and for each element  $\alpha \in B_n$ ,  $E_h^n$  contains an edge from  $(v, \alpha)$  to  $(u, \alpha h(\bar{e}))$ , where  $\bar{e}$  is the projection of  $e$  to  $\mathcal{UC}_n$  by natural surjection, and  $h(\bar{e})$  is calculated using the method described in § 4.4.

It is important to note that, for a specific multi-agent path planning task, it is not necessary to construct the entire graph as it is not connected. Instead, we can focus on the relevant connected components of the graph. For example, for any vertex  $v \in V^n$  and elements  $\alpha, \beta \in B_n$ , the connected components of  $(v, \alpha)$  and  $(v, \beta)$  are different unless  $\alpha^{-1}\beta \in P_n$ .

With our approach, we represent the homotopy classes of solutions for a specific instance of the labeled multi-agent path planning problem by labeling them with elements in a coset of the pure braid group, instead of those in the pure braid group. The choice of coset depends on the relative positions of the agents' start and goal locations. For a detailed explanation of why we do not use the pure braid group, see Appendix A.

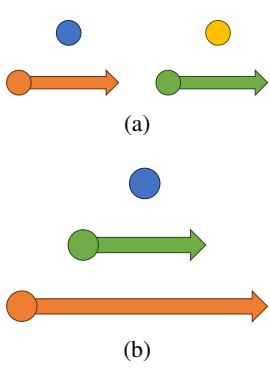


Figure 5: Figures illustrating relations

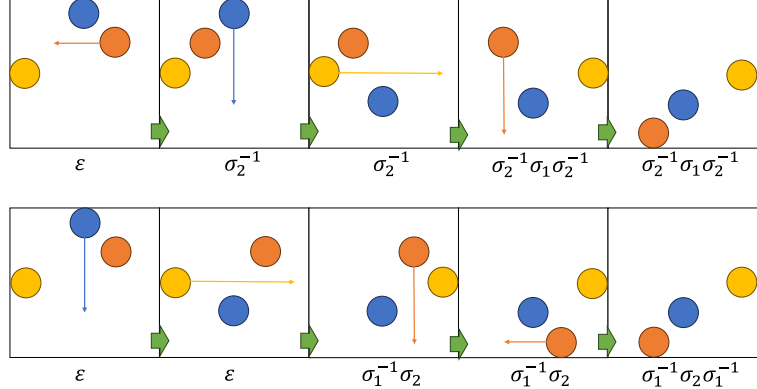


Figure 6: Examples of braid construction

#### 4.4 Word Construction

The construction of words for  $\mathcal{UC}_n$  is classically known [Fox and Neuwirth, 1962].

Let  $p_1 = (x_1, y_1), \dots, p_n = (x_n, y_n)$  be the natural coordinates of  $\mathcal{C}_n$ . We define:

$$\lambda_{2n} := \{x_1 < x_2 < \dots < x_n\}, \quad (9)$$

$$\lambda_i^{2n-1} := \{x_1 < \dots < x_i = x_{i+1} < \dots < x_n, y_i < y_{i+1}\}, \quad (10)$$

for  $1 \leq i < n$ . It is easy to see that the map  $\lambda^{2n} \cup \bigcup_i \lambda_i^{2n-1} \hookrightarrow \mathcal{C}_n \rightarrow \mathcal{UC}_n$  is injective. We identify  $\lambda^{2n}, \lambda_i^{2n-1}$  with their images.  $\mathcal{UC}_n \setminus \lambda^{2n}$  is  $(2n - 1)$ -dimensional and  $\mathcal{UC}_n \setminus \lambda^{2n} \setminus \bigcup_i \lambda_i^{2n-1}$  is  $(2n - 2)$ -dimensional.

For simplicity, we assume that all  $v \in V^n$  lie on  $\lambda^{2n}$ . We also choose a base point  $x_0$  of the fundamental group within  $\lambda^{2n}$ . To make the homotopy-augmented graph explicit, we choose the standard path connecting  $x_0$  and vertices of  $V^n$  in  $\lambda^{2n}$ . The generator  $\sigma_i$  of  $\pi_1(\mathcal{UC}_n) = B_n$  is represented by a loop in  $\lambda^{2n} \cup \lambda_i^{2n-1}$  that traverses  $\lambda_i^{2n-1}$  exactly once with the direction from region  $\{y_i < y_{i+1}\}$  to region  $\{y_i > y_{i+1}\}$ . Consequently, for an edge  $e$  on  $\mathcal{UC}_n$ , the word representing the corresponding braid  $h(e)$  is constructed by detecting the traverses of  $e$  with  $\lambda_1^{2n-1}, \dots, \lambda_{n-1}^{2n-1}$ . By examining the intersections of the boundaries of  $\lambda_1^{2n-1}, \dots, \lambda_{n-1}^{2n-1}$ , we obtain the relations  $\sigma_i \sigma_j = \sigma_j \sigma_i$  for  $i + 1 < j$  and  $\sigma_i \sigma_{i+1} \sigma_i = \sigma_{i+1} \sigma_i \sigma_{i+1}$ . Detailed derivations of these relations are omitted for brevity.

Intuitively, this construction can be described as follows. We number the agents in ascending order of their  $x$ -coordinates.  $\sigma_i$  corresponds to the counterclockwise swap (Figure 1a) of the agent with number  $i$  and the agent with number  $(i + 1)$ , and  $\sigma_i^{-1}$  corresponds to their clockwise swap (Figure 1b). The word for an edge is constructed by detecting the swaps of agent indexes. The graphical explanation for the relations is shown in Figure 5. The left or bottom agent represents the  $i$ -th agent, and the other agent represents either the  $j$ -th agent ( $j > i + 1$ , in (a)) or the  $(i + 1)$ -th agent (in (b)). The movement of agents is depicted with arrows. The key observation is that the order in which the agents move does not affect the homotopy class. Therefore, we have two relations: (a)  $\sigma_i \sigma_j = \sigma_j \sigma_i$  and (b)  $\sigma_i \sigma_{i+1} \sigma_i = \sigma_{i+1} \sigma_i \sigma_{i+1}$ .

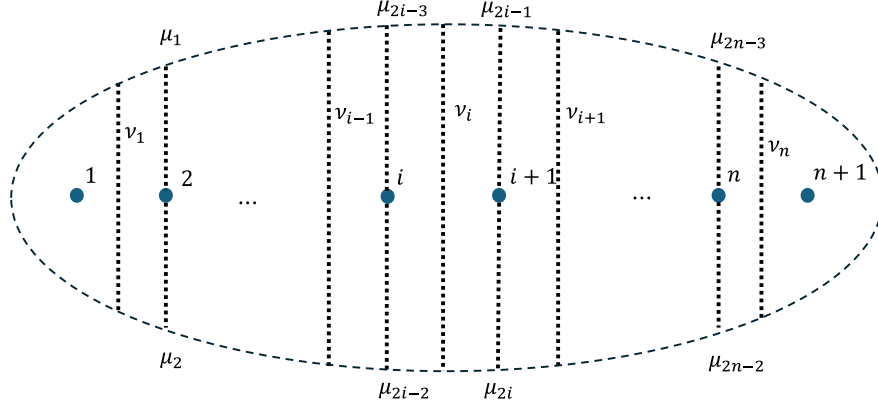
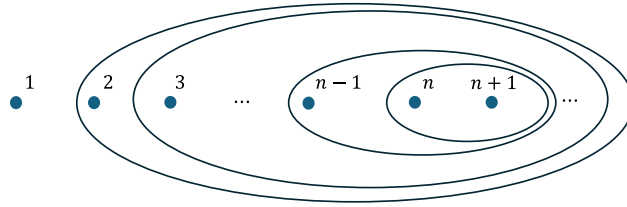
Figure 6 shows two examples of word construction. In the top example, the agents with numbers 2 and 3 swap clockwise at the first block, then the agents with numbers 1 and 2 swap counterclockwise and the agents with numbers 2 and 3 swap clockwise at the third block. In the example below, the agents with numbers 1 and 2 swap clockwise and the agents with numbers 2 and 3 swap counterclockwise at the second block; then, the agents with numbers 1 and 2 swap clockwise at the fourth block.

#### 4.5 Dynnikov Coordinates

We follow the description in Thiffeault [2022].

Intuitively, Dynnikov coordinates represent a multicurve on a plane with aligned  $n + 1$  holes.<sup>7</sup> Here, ‘‘multicurve’’ means a disjoint union of simple closed curves, any of which encircles at least two holes but not all of them. For an example, see the example calculation at the end of this subsection. Figure 7 illustrates a plane with holes, where symbols attached to lines or half lines indicate the number of times the multicurve intersects them. Holes are numbered

<sup>7</sup>While  $n$  holes are enough to define the action by  $B_n$ , this action is not faithful.

Figure 7: Plane with  $n + 1$  holesFigure 8: Multicurve corresponding to  $u$ 

from left to right. For  $2 \leq i \leq n$ ,  $\mu_{2i-3}$  and  $\mu_{2i-2}$  correspond to the half lines extending up and down from the  $i$ -th hole, respectively. For  $1 \leq i \leq n$ ,  $\nu_i$  corresponds to the vertical line between the  $i$ -th and  $i + 1$ -th holes. When counting the numbers of intersections, we take the minimum ones, allowing for homotopical deformation of curves.

For any  $1 \leq i \leq n - 1$ , let

$$a_i := \frac{\mu_{2i} - \mu_{2i-1}}{2},$$

$$b_i := \frac{\nu_i - \nu_{i+1}}{2}.$$

Then,  $(a_1, \dots, a_{n-1}, b_1, \dots, b_{n-1})$  gives a bijection between homotopy classes of multicurves and  $\mathbb{Z}^{2n-2} \setminus \{\mathbf{0}\}$ , that is *Dynnikov coordinates* [Hall and Yurttas, 2009].

The braid group  $B_{n+1}$  acts on the homotopy classes of multicurves by moving holes. For an example, again, see the example calculation at the end of this subsection. Here, we are only interested in the action of  $B_n$  as a subgroup of  $B_{n+1}$ . The action of  $B_n$  can be written using Dynnikov coordinates as follows. For  $x \in \mathbb{Z}$ , we write  $x^+ := \max\{x, 0\}$  and  $x^- := \min\{x, 0\}$ . For  $i = 1, \dots, n-1$  and  $e = \pm 1$ , we can calculate  $(a'_1, \dots, a'_{n-1}, b'_1, \dots, b'_{n-1}) := (a_1, \dots, a_{n-1}, b_1, \dots, b_{n-1}) \cdot \sigma_i^e$  as

$$(a'_k, b'_k) := \begin{cases} (-b_1 + (a_1 + b_1^+)^+, a_1 + b_1^+) & \text{for } i = k = 1, e = +1, \\ (b_1 - (b_1^+ - a_1)^+, b_1^+ - a_1) & \text{for } i = k = 1, e = -1, \\ (a_{i-1} - b_{i-1}^+ - (b_i^+ + c)^+, b_i + c^-) & \text{for } i > 1, k = i - 1, e = +1, \\ (a_{i-1} + b_{i-1}^+ + (b_i^+ - d)^+, b_i - d^+) & \text{for } i > 1, k = i - 1, e = -1, \\ (a_i - b_i^- - (b_{i-1}^- - c)^-, b_{i-1} - c^-) & \text{for } i > 1, k = i, e = +1, \\ (a_i + b_i^- + (b_{i-1}^- + d)^-, b_{i-1} + d^+) & \text{for } i > 1, k = i, e = -1, \\ (a_k, b_k) & \text{for } k \neq i - 1, i, \end{cases} \quad (11)$$

where  $c := a_{i-1} - a_i - b_i^+ + b_{i-1}^-$  and  $d := a_{i-1} - a_i + b_i^+ - b_{i-1}^-$  [Thiffeault, 2022].

Moreover, where  $u := (a_1 = 0, \dots, a_{n-1} = 0, b_1 = -1, \dots, b_{n-1} = -1) \in \mathbb{Z}^{2n-2}$ , which corresponds to the multicurves in Figure 8, for any  $\alpha, \beta \in B_n$ ,  $u \cdot \alpha = u \cdot \beta$  if and only if  $\alpha = \beta$  [Dynnikov, 2002, Thiffeault, 2022]. Thus, we can represent an element  $\alpha$  in  $B_n$  by  $u \cdot \alpha \in \mathbb{Z}^{2n-2} \setminus \{\mathbf{0}\}$ .

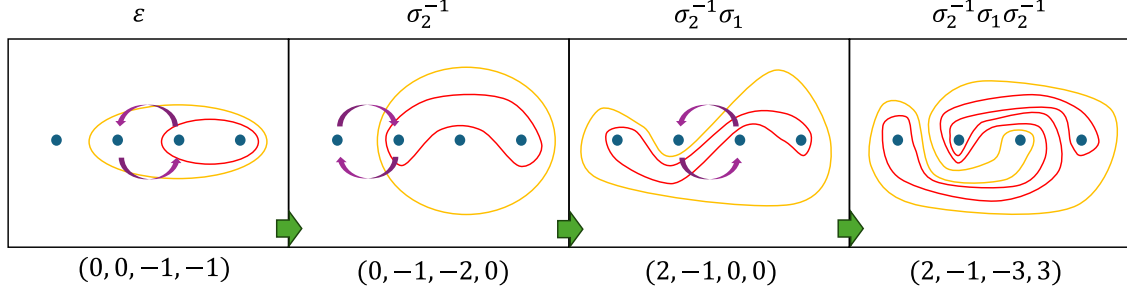
Figure 9: Action of  $\sigma_2^{-1}\sigma_1\sigma_2^{-1}$  and Dynnikov coordinates

Figure 9 shows examples of the action of the braid group and Dynnikov coordinates when  $n = 3$ . The top shows braids, the middle shows multicurves after these braids acted on  $u$ , and the bottom shows the corresponding Dynnikov coordinates. The Dynnikov coordinates corresponding to  $\sigma_2^{-1}\sigma_1\sigma_2^{-1}$  are  $(2, -1, -3, 3)$ .

#### 4.6 Revised Prioritized Planning

We adopt *revised prioritized planning* (RPP) [Čáp et al., 2015] for pathfinding. As classical prioritized planning, we fix a predetermined priority order for the agents and proceed to plan their paths one by one, avoiding collisions with the paths of previously planned agents. In RPP, in addition, the start positions of agents that have not yet been planned are also avoided, ensuring the completeness of the planning process under certain assumptions.

Algorithm 1 presents the pseudocode of our homotopy-aware version of RPP, which generates homotopically distinct solutions. The notation  $\varepsilon$  denotes the Dynnikov coordinates corresponding to the empty braid. At line 8, we construct a graph  $G_{plan}$ , which is created by adding a time dimension to  $G$  and removing parts colliding with  $plan$ , the same as Silver [2005].<sup>8</sup> In this construction, we also remove  $s_{i+1}, \dots, s_n$  from  $G_{plan}$ . (Strictly speaking, we allow an agent to reach one of such positions if the position is its goal, since it cannot finish otherwise.) In the following lines,  $s_{plan}$  and  $g_{plan}$  denote the vertices corresponding to the start, which is  $s_i$  with time 0, and the goal, which is  $g_i$  with a late enough time, respectively. At line 14, the popped element  $(plan, v, w)$  is selected as that with the minimum  $\text{cost}(plan) + D[plan, v, w] + h(v, g_{plan})$ , where  $h$  is the heuristic function.

The function  $\text{NextBraid}(plan, e, w)$  at line 24 returns the Dynnikov coordinates updated from  $w$  after the agent  $i$  moves along  $e$  and the agents from 1 to  $i - 1$  move in accordance with  $plan$ . It is calculated as follows. First, as explained in § 4.4, the swaps of the order of the agents'  $x$ -coordinates by these moves are enumerated. Second, for each swap, the Dynnikov coordinates are updated by (11) in order.

For simplicity, we omit the details on path reconstruction.

*Remark 3.* While we adopt the RPP approach for scalability in this paper, we can also solve the  $k$ -shortest non-homotopic path planning [Bhattacharya and Ghrist, 2018, Yang et al., 2022] by A\* searching the homotopy-augmented graph.

#### 4.7 Completeness

As RPP in the classical case, we can prove the completeness of the algorithm under some specific condition for problem instances. Note that this does not mean that our algorithm is practical only for such cases.

Before the completeness proposition, we state a lemma used in the proof.

**Lemma 4.** For any  $1 \leq k \leq n$ , let  $F_k : P_n \rightarrow P_{n-1}$  be the projection forgetting the  $k$ -th strand. For  $1 \leq i < j \leq n$ , let

$$a_{i,j} := \sigma_{j-1}\sigma_{j-2}\cdots\sigma_{i+1}\sigma_i^2\sigma_{i+1}^{-1}\cdots\sigma_{j-2}^{-1}\sigma_{j-1}^{-1} = \sigma_i^{-1}\sigma_{i+1}^{-1}\cdots\sigma_{j-2}^{-1}\sigma_{j-1}^2\sigma_{j-2}\cdots\sigma_{i+1}\sigma_i \in P_n. \quad (12)$$

Then, the kernel of  $F_k$  is generated by  $a_{1,k}, a_{2,k}, \dots, a_{k-1,k}$  and  $a_{k,k+1}, a_{k,k+2}, \dots, a_{k,n}$ .

*Proof.* This is true for  $k = n$  [Rolfsen, 2010]. For arbitrary  $k$ , let  $b_k := \sigma_{n-1}\sigma_{n-2}\cdots\sigma_k \in B_n$ . Since  $P_n$  is a normal subgroup, the conjugation by  $b_k$  maps  $P_n$  to  $P_n$ . Furthermore,  $F_k(\alpha) = F_n(b_k\alpha b_k^{-1})$ . Thus, the kernel of  $F_k$

<sup>8</sup>If continuous time is considered, you can use the method in Phillips and Likhachev [2011].

**Algorithm 1** Homotopy-Aware RPP

---

```

1: Input a graph  $G = (V, E)$ 
2: Input starts and goals  $(s_1, g_1), \dots, (s_n, g_n)$ 
3:  $plans \leftarrow \{\emptyset\}$ 
4: for  $i = 1, \dots, n$  do
5:    $Open, Closed \leftarrow \emptyset, \emptyset$ 
6:   Initialize a map  $D$ 
7:   for  $plan \in plans$  do
8:     Construct timed graph  $G_{plan} = (V_{plan}, E_{plan})$ 
9:     Insert  $(plan, s_{plan}, \epsilon)$  to  $Open$ 
10:     $D[plan, s_{plan}, \epsilon] \leftarrow 0$ 
11:   end for
12:    $newplans \leftarrow \emptyset$ 
13:   while  $Open \neq \emptyset$  do
14:     Pop  $(plan, v, w)$  from  $Open$ 
15:     Insert  $(plan, v, w)$  to  $Closed$ 
16:     if  $v = g_{plan}$  then
17:       Reconstruct path  $p$  of agent  $i$ 
18:       Insert  $plan \cup p$  to  $newplans$ 
19:       if enough plans are found then
20:         break
21:       end if
22:     end if
23:     for edge  $e \in E_{plan}$  from  $v$  do
24:        $v', w', d' \leftarrow \text{target}(e), \text{NextBraid}(plan, e, w), D[plan, v, w] + \text{length}(e)$ 
25:       if  $(plan, v', w') \notin Open \cup Closed$  then
26:          $D[plan, v', w'] \leftarrow d'$ 
27:         Insert  $(plan, v', w')$  to  $Open$ 
28:       else if  $D[plan, v', w'] > d'$  then
29:          $D[plan, v', w'] \leftarrow d'$ 
30:       end if
31:     end for
32:   end while
33:    $plans \leftarrow newplans$ 
34: end for
35: return  $plans$ 

```

---

is generated by  $b_k^{-1} a_{1,n} b_k, \dots, b_k^{-1} a_{n-1,n} b_k$ , which can be calculated as

$$b_k^{-1} a_{i,n} b_k = \begin{cases} a_{i,k} & \text{if } i < k \\ a_{k,i+1} & \text{if } i \geq k. \end{cases} \quad (13)$$

□

Intuitively, the following proposition says that our algorithm is complete when the obstacles and start and goal positions are separated enough with respect to the size of the agents.

**Proposition 5.** *We assume the following conditions:*

- *An agent moving along the boundary of  $\mathcal{D}$  never collides with obstacles or other agents staying at  $s_1, \dots, s_n, g_1, \dots, g_n$ , or  $s_{i+1}, \dots, s_n$ .*
- *For any  $1 \leq i \leq n$ , there exists a loop around  $g_i$  in  $\mathcal{D}$  such that it does not enclose any obstacle, other goal position, or  $s_j$  with  $j > i$ , and an agent moving along it never collides with obstacles or other agents staying at any goal position or  $s_j$  with  $j > i$ .*
- *For any  $1 \leq i \leq n$ , there exists a loop around  $s_i$  such that it does not enclose any obstacle, other start position, or  $g_j$  with  $j < i$ , and an agent moving along it never collides with obstacles or other agents staying at any start position or  $g_j$  with  $j < i$ .*

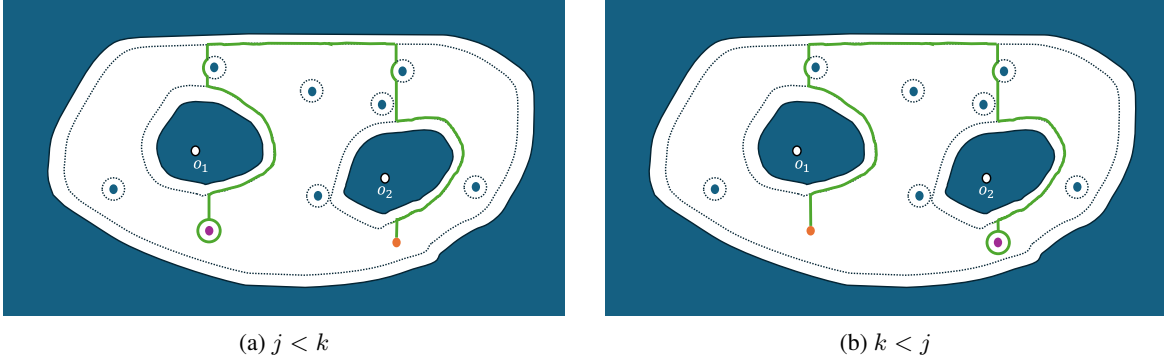


Figure 10: Paths with homotopy corresponding to  $a_{j,k}$ ,  $a_{k,j}$  or its inverses. The circle enclosed by the path means  $g_i = c_j$  and the circle at the endpoint of the path means  $c_k$ . Other circles mean other  $c_1, \dots, c_i$  or  $s_{i+1}, \dots, s_n$ .

Then, when the roadmap  $G$  is dense enough, for any homotopy class of solutions, Algorithm 1 can provide a solution belonging to it.

*Proof.* We consider a problem instance  $(s_1, g_1), \dots, (s_n, g_n)$  satisfying the assumption and a braid  $\alpha \in B_{r+n}$  corresponding to one of its solutions. For  $0 \leq i \leq n$ , let  $\alpha_i \in B_{r+i}$  be the braid corresponding to the paths for the first  $i$  agents in  $\alpha$ . We prove that our method can generate a solution  $p_i$  in the homotopy class corresponding to  $\alpha_i$  by induction for  $i$ . When  $i = 0$ , this is clear because no agent is considered, and  $\alpha_0$  is the unit.

For  $i \geq 1$ , under the assumption of the problem instance, the  $i$ -th agent can reach its goal after agents from 1 to  $i - 1$  have finished while avoiding the goal positions  $g_1, \dots, g_{i-1}$  and the start positions  $s_{i+1}, \dots, s_n$ . Therefore, we can generate a plan  $p'_i$  for the first  $i$  agents on the basis of  $p_{i-1}$ . Let  $\beta_i \in B_{r+i}$  be the braid corresponding to  $p'_i$ .

To construct the desired plan, we need to add the moves of the  $i$ -th agent after  $p'_i$ . These moves must correspond to the braid  $\beta_i^{-1} \alpha_i \in B_{r+i}$ . Let  $c_1, \dots, c_{r+i}$  be  $o_1, \dots, o_k, g_1, \dots, g_i$  sorted by their  $x$ -coordinates, and suppose  $g_i = c_k$  ( $1 \leq k \leq r + i$ ). Since  $\alpha_i$  and  $\beta_i$  coincide when the  $i$ -th agent is forgotten,  $\beta_i^{-1} \alpha_i$  is in the kernel of  $F_k$ , which is generated by  $a_{1,k}, \dots, a_{k-1,k}, a_{k,k+1}, \dots, a_{k,r+i}$  as previously proved.

Thus, it is sufficient to demonstrate that, after all  $i$  agents have reached their goals, the  $i$ -th agent can move to construct any of  $a_{1,k}, \dots, a_{k-1,k}, a_{k,k+1}, \dots, a_{k,r+i}$  and their inverses, while avoiding  $g_1, \dots, g_{i-1}$  and  $s_{i+1}, \dots, s_n$ .

For  $1 \leq j < k$ , the agent first moves up (in the positive direction of the  $y$ -axis) avoiding obstacles,  $g_1, \dots, g_{i-1}$ , and  $s_{i+1}, \dots, s_n$  by moving partially along the boundaries or the assumed loops. When avoiding the obstacle  $O_l$ , if the  $x$  coordinate of  $o_l$  is smaller than that of  $c_k$ , it avoids to the right (the positive side of the  $x$ -axis); otherwise, it avoids to the left. This is the same for  $g_1, \dots, g_{i-1}$ . Then, the agent moves to the left until it reaches the same  $x$ -coordinate as  $c_j$  along the outside boundary and moves down to  $c_j$  avoiding obstacles and other start or goal positions. When going down as well as going up, the agents avoid obstacles or goal positions represented by  $c_l$  to the right (from our point of view) if the  $x$ -coordinate of  $c_l$  is smaller than that of  $c_j$ ; otherwise, it avoids to the left. It circumvents  $c_j$  counterclockwise or clockwise and returns to  $c_k$  using the same path. The braid for such a loop is given by:

$$\sigma_{k-1} \cdots \sigma_{j+1} \sigma_j^{\pm 2} \sigma_{j+1}^{-1} \cdots \sigma_{k-1}^{-1} = a_{j,k}^{\pm 1}, \quad (14)$$

where the sign depends on the direction for moving around  $c_j$ . Similarly, for  $k < j \leq n$ , the agent follows the path described above in reverse order to  $c_j$ , around  $c_j$ , and back. The braid is given by:

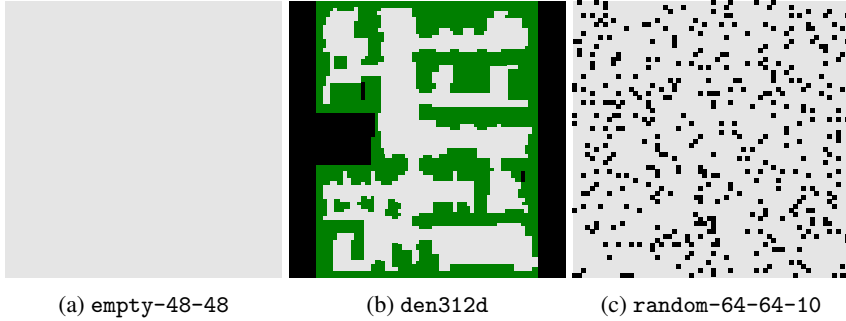
$$\sigma_k^{-1} \cdots \sigma_{j-2}^{-1} \sigma_{j-1}^{\pm 2} \sigma_{j-2} \cdots \sigma_k = a_{k,j}^{\pm 1}. \quad (15)$$

Figure 10 illustrates examples of such paths.

When the roadmap is dense enough, these paths can be approximated by paths on the graph.  $\square$

In particular, in the case of the grid, by the construction of paths in the proof, the following corollary holds. To facilitate the word construction method in grid environments, we introduce a virtual slightly inclined  $x$ -axis, such that for any two grid cells  $(i, j)$  and  $(k, l)$ , cell  $(i, j)$  has a smaller  $x$ -coordinate than cell  $(k, l)$  if and only if  $i < k$  or  $i = k, j < l$ .

**Corollary 6.** We consider cases where  $\mathcal{D}$  is a region composed of grids, and  $G$  is a four-connective grid graph. We assume the following conditions:



(a) empty-48-48

(b) den312d

(c) random-64-64-10

Figure 11: Maps for evaluation of runtime

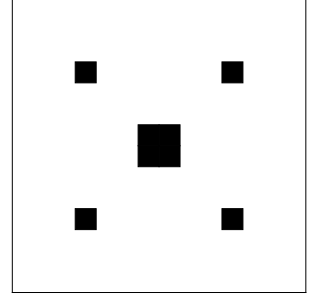


Figure 12: Grid map with five obstacles

- No start grid or goal grid is adjacent to obstacle grids vertically, horizontally, or diagonally.
- No two start grids or two goal grids are adjacent vertically, horizontally, or diagonally.
- For any  $1 \leq i < j \leq n$ ,  $g_i$  and  $s_j$  are not adjacent vertically, horizontally, or diagonally.

Then, for any homotopy class of solutions, Algorithm 1 can provide a solution belonging to it.

## 5 Experiments

We conducted two experiments. In the first experiment, we measured the runtime of our method to assess its scalability, comparing it with that of a method using the Dehornoy order and the handle reduction algorithm [Dehornoy, 1997] instead of Dynnikov coordinates. In the second experiment, our focus was to demonstrate the effectiveness of generating homotopically distinct coarse solutions for planning low-cost trajectories. We demonstrate how our approach can lead to improved trajectories by comparing the results obtained after optimization. The codes used for these experiments are available at <https://github.com/omron-sinix/homotopy-aware-MAPP>.

### 5.1 Problem Setting and Implementation

For both experiments, we used problem instances of multi-agent pathfinding on grids. As is common practice, we forbid vertex conflicts, where two agents occupy the same grid cell, and swapping conflicts, where two agents move along the same edge in opposite directions at the same time [Stern et al., 2019].

In our implementation, we precomputed the minimum distance to  $g_{plan}$  for all vertices of  $G_{plan}$  and adopted it as the heuristic function  $h$ . Line 19 of Algorithm 1 checks whether the desired number ( $K$ ) of solutions has been found. Our implementation was conducted in C++, and we used the priority queue and map data structures from the standard library to manage *Open*, *Closed*, and *D*. Dynnikov coordinates were implemented by using the GMP library.

We used Intel(R) Xeon(R) Gold 6338 CPUs @ 2.00 GHz for these experiments.

### 5.2 Evaluation of Runtime

We ran our method (**Dyn**) with the objective of finding 100 solutions. The runtime from the beginning was measured after each agent’s planning process was completed (line 33 in Algorithm 1).

#### 5.2.1 Problem Instances

We evaluated the runtime performance using random instances of the multi-agent pathfinding problem. We used the three grid maps, empty-48-48, den312d, and random-64-64-10, illustrated in Figure 11, from Moving AI MAPP Benchmarks [Stern et al., 2019] as environments. The sizes of the maps were  $48 \times 48$ ,  $81 \times 65$ , and  $64 \times 64$ , respectively. The numbers of the connected components of obstacles ( $r$  in the previous section) were 0, 4, and 241, respectively. We generated 10 instances with 500 agents on each map. To ensure at least some solutions can be found, we imposed a condition on problem instances that guaranteed that the classical RPP would find a solution, i.e., for any  $1 \leq i < n$ , the agent  $i$  can reach the goal without visiting  $s_{i+1}, \dots, s_n$  or  $g_1, \dots, g_{i-1}$ .

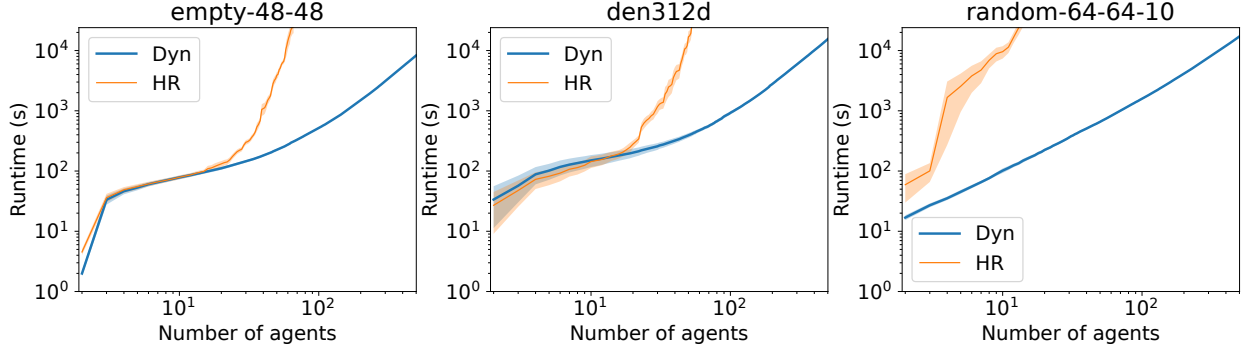


Figure 13: Log-log plots of runtime with colored areas representing standard errors

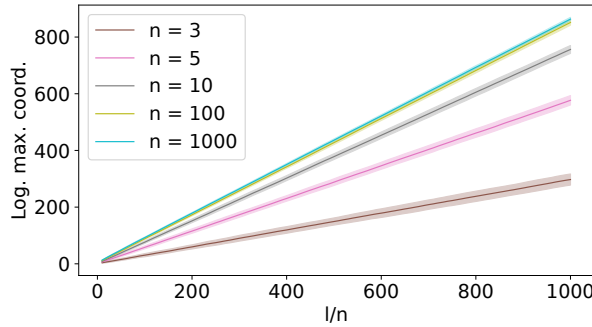


Figure 14: Logarithms of coordinates for random braids with colored areas representing standard derivations

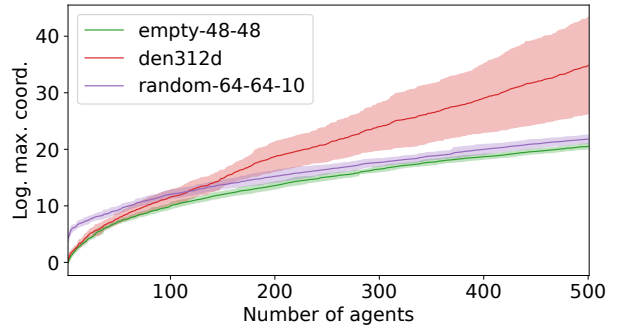


Figure 15: Logarithms of coordinates in experiments with colored areas representing standard derivations

### 5.2.2 Baseline

We also recorded the maximum absolute value of the Dynnikov coordinates for the first generated solution at the same time. For comparison, we also ran a method (**HR**) that is the same with ours except that it uses the Dehornoy order [Dehornoy, 1994] to maintain braids and the handle-reduction algorithm [Dehornoy, 1997] to determine the order. More precisely, we used the “FullHRed” algorithm as a specific strategy for the handle reduction method.

### 5.2.3 Results and Discussion

Figure 13 illustrates the results of the runtimes, which show that the runtime order of with respect to the number  $n$  of agents was smaller for our method than for **HR**. Moreover, while the runtime increased significantly in the case with many obstacles (random-64-64-10) compared with the other cases in **HR**, it did not change much in our method.

In the case of the empty map, the runtime of **HR** was approximately  $\Theta(n^5)$ , which means that the runtime for the planning for the  $n$ -th agent was  $\Theta(n^4)$ . This is expected when the handle reduction is the bottleneck because the lengths  $l$  of braid words are expected to be roughly  $\Theta(n^2)$  and the time complexity of the handle reduction method is conjectured to be  $\Theta(l^2)$  [Dehornoy et al., 2008].

On the other hand, the runtime order of our method seemed to be roughly  $\Theta(n^2)$ , which was smaller than the expected order explained below for calculating Dynnikov coordinates, which means that this calculation was not a bottleneck at the scale of our experiment. Indeed, when we profiled the performance of a single run by using gprof, comparison and update of Dynnikov coordinates accounted for 7.2% and 12.3% of runtime, respectively, even in random-64-64-10.

The complexity of one update calculation (11) was  $\Theta(\log X)$ , where  $X$  is the absolute value of the coordinates. While  $\log X$  is bounded as  $O(l)$ , where  $l$  is a length of the braid word, for arbitrary words, it is expected to be  $\Theta(l/n)$ , where  $n$  is the number of strands, for random words. To confirm this, we generated 100 random braid words with a length of  $1000n$  for each value of  $n = 3, 5, 10, 100, 1000$  and calculated the maximum absolute values of the Dynnikov coordinates. The results shown in Figure 14 demonstrate that the expected value of  $\log X$  is linear to  $l/n$  and that the coefficient is independent of  $n$  when  $n$  is large enough.

In our method, since the expected lengths of braid words for the planning of the  $n$ -th agent is roughly  $\Theta(n^2)$ ,  $\log X$  is expected to be  $\Theta(n)$ , which is consistent with the plot of the logarithms of the maximum absolute values of coordinates with respect to  $n$  as shown in Figure 15 when  $n$  is enough large. On the other hand, this figure also shows that the coefficients vary depending on the shapes of maps and are larger for complex maps such as den312d. The number of update calculations for the planning for the  $n$ -th agent is roughly estimated to be  $\Theta(n^2)$ , so the runtime for the planning for the  $n$ -th agent is expected to be  $\Theta(n^3)$ . Thus, the total runtime for calculating Dynnikov coordinates for the planning of  $n$  agents is expected to be  $\Theta(n^4)$ . When the number of agents is much larger, this cost will dominate.

### 5.3 Optimization Experiment

To confirm that generating multiple homotopically distinct solutions contributes to finding better trajectories after optimization, we performed the following experiments. First, for instances on grid maps, we generated multiple solutions on grids by using our method and baseline methods. Next, we continuously optimized the found solutions and compared the costs of the optimized trajectories.

#### 5.3.1 Problem Instances

We used two small grid maps: an empty  $14 \times 14$  map and a handmade map of the same size with five obstacles as shown in Figure 12. For each map, we generated 100 problem instances with start positions selected at random to be distinct and similarly selected goal positions. For each instance, we generated 100 homotopically distinct solutions with our method.

#### 5.3.2 Baselines

We also generated initial solutions using two approaches as baseline methods:

- **Optimal one (OO):** We generated one optimal solution on the grid for each instance.
- **Revised prioritized planning with various priority orders (PPvP):** We generated 100 solutions for each instance by revised prioritized planning with randomly selected priority orders.

#### 5.3.3 Optimization Method

After generating the initial solutions, we proceeded to optimize them. Let  $\gamma_1, \dots, \gamma_n$  be the trajectories of the agents. The cost function  $C$  is defined as

$$C(\gamma_1, \dots, \gamma_n) := \frac{1}{2} \sum_i \int_0^1 \left\| \frac{d^2 \gamma_i}{dt^2}(t) \right\|^2 dt + c_c \sum_{i \neq j} \int_0^1 \max \left\{ \frac{1}{\|\gamma_i(t) - \gamma_j(t)\|} - \frac{1}{2r}, 0 \right\}^2 dt + c_c \sum_{i=1}^n \sum_{l=0}^r \int_0^1 \max \left\{ \frac{1}{d_l(\gamma_i(t))} - \frac{1}{r}, 0 \right\}^2 dt \quad (16)$$

with constraints

$$\frac{d\gamma_i}{dt}(0) = \frac{d\gamma_i}{dt}(1) = \mathbf{0}, \quad (17)$$

where  $c_c$  is a penalty coefficient,  $r = \sqrt{2}/4$  is the collision radius of agents<sup>9</sup>, and  $d_l$  means the distance from  $O_l$  for  $l > 0$  and that from the outside boundary for  $l = 0$ . The first term represents a smoothness cost [Zucker et al., 2013], while the second and third terms represent a collision penalty [Kasaura et al., 2023].

More precisely, we approximate the trajectories of the  $i$ -th agent by  $(L + 1)$  timed waypoints  $(p_{i,0}, 0), (p_{i,1}, 1/L), \dots, (p_{i,L}, 1)$  with  $p_{i,0} = s_i$  and  $p_{i,L} = g_i$ , where  $L = 100$ . The cost function is then

<sup>9</sup>This is the maximum radius at which no collisions occur in solutions on grid maps.

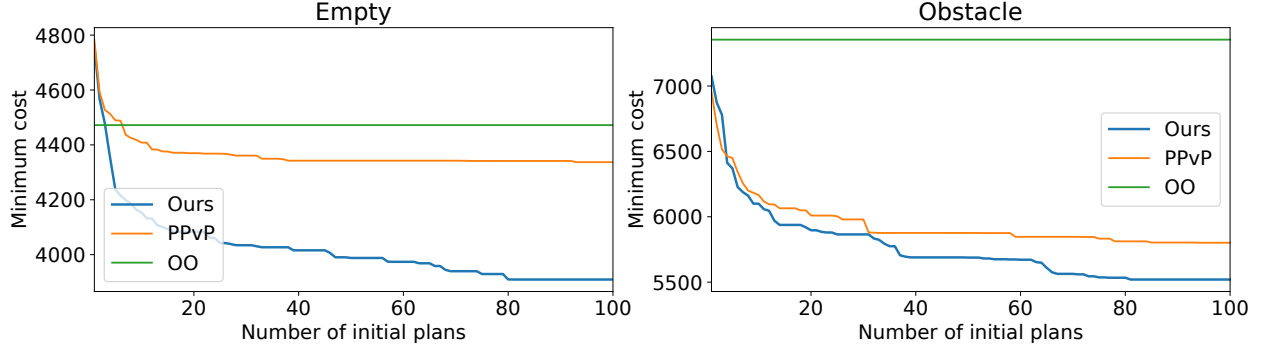


Figure 16: Minimum cost of plans after optimization among first  $N$  generated plans, averaged over 100 instances, with respect to  $N$

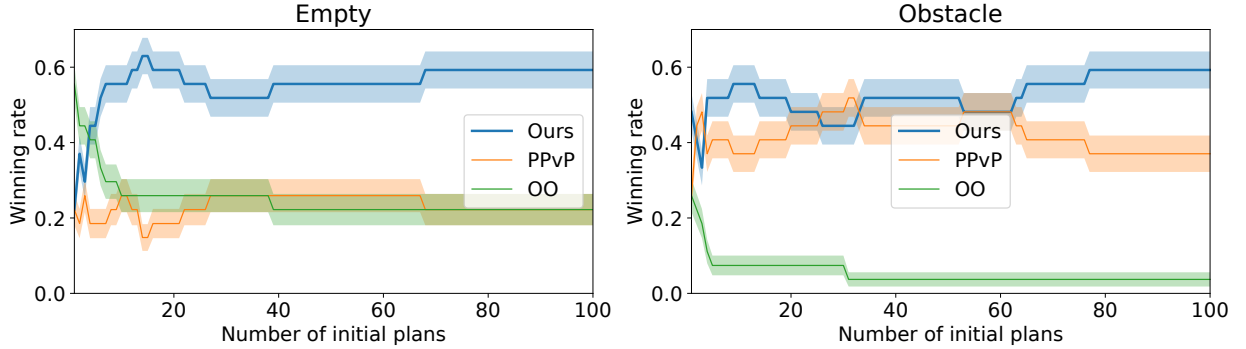


Figure 17: Winning rates with colored areas representing standard errors

reformulated as

$$\begin{aligned}
 C(p_{1,0}, \dots, p_{1,L}, p_{2,0}, \dots, p_{n,L}) := & \frac{L^3}{2} \sum_i \sum_{k=0}^{L-1} \|p_{i,k+1} + p_{i,k-1} - 2p_{i,k}\|^2 \\
 & + \frac{c_c}{L} \sum_{i \neq j} \sum_{k=0}^{L-1} \max \left\{ \frac{1}{\|p_{i,k} - p_{j,k}\|} - \frac{1}{2r}, 0 \right\}^2 \\
 & + \frac{c_c}{L} \sum_{i=1}^n \sum_{l=0}^r \sum_{k=0}^{L-1} \max \left\{ \frac{1}{d_l(p_{i,k})} - \frac{1}{r}, 0 \right\}^2,
 \end{aligned} \tag{18}$$

where  $p_{i,-1} := p_{i,0}$  and  $p_{i,L+1} := p_{i,L}$ . We solved this continuous optimization problem with the Levenberg-Marquardt [Levenberg, 1944, Marquardt, 1963] algorithm implemented in  $g^2o$  1.0.0 [Kümmerle et al., 2011]. The  $p_{i,k}$  values were initialized by the initial plan on the grid. We optimized them with 10000 steps of the Levenberg-Marquardt algorithm. The collision-penalty constant  $c_c$  was initially set to  $10^6$  and multiplied by 1.001 after every optimization step.

### 5.3.4 Results and Discussion

In Figure 16, for each value of  $N = 1, \dots, 100$  on the  $x$ -axis, the curve labeled **Ours** and the curve labeled **PPvP** represent the cost of the best plan obtained from optimizing the first  $N$  initial plans, averaged over 100 instances. The line labeled **OO** represents the cost of optimization of the optimal plan on the grid, also averaged over 100 instances. Figure 17 shows the winning rates. For each method, the curve represents the percentage of instances where the best plan among the first  $N$  plans of all methods is generated by it, where  $N = 1, \dots, 100$ . If costs are the same, the instance is counted for both methods.

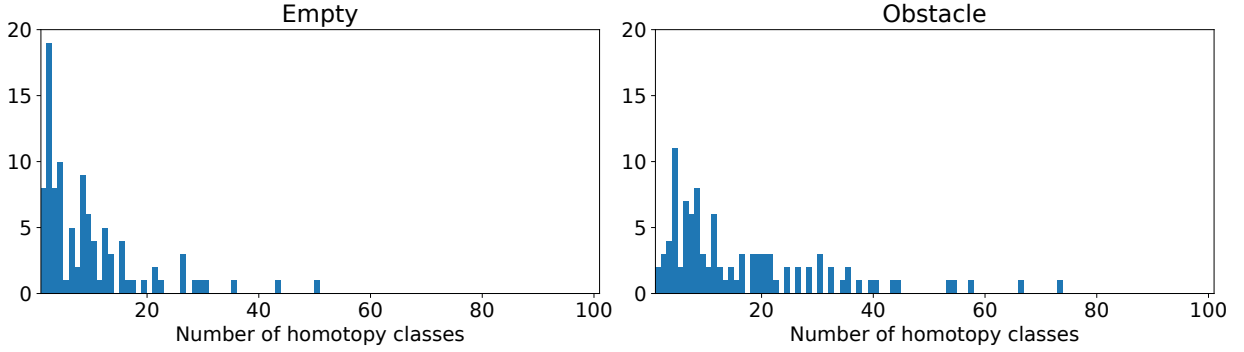


Figure 18: Number of homotopy classes present in 100 solutions generated with **PPvP** for each 100 instances

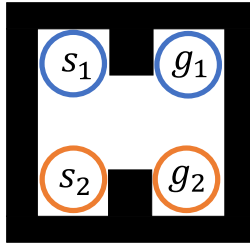


Figure 19: Example scenarios in which homotopy depends on order in which agents pass through narrow part

While, in the empty map, **OO** tended to produce the best trajectories when only a few initial solutions were considered, it seems strange that **OO** was not the best even at  $N = 1$  in the map with obstacles. This may be because reducing costs by making clever moves on narrow parts of the grid would make the optimized trajectories worse.

For both maps, **Ours** tended to produce better solutions than **PPvP** in terms of both average cost and winning rate. The difference was larger for the empty map than for the map with obstacles. We counted the number of homotopically distinct solutions generated with **PPvP** for each instance. The distribution is shown in Figure 18 as histograms. The results indicate that **PPvP** generated few homotopies, especially on the empty map. This is natural given the lack of homotopy divergence due to obstacles on the empty map. Thus, our method is particularly effective on maps with few obstacles, where it is difficult to generate homotopically distinct plans naively.

## 6 Conclusion and Future Work

We proposed a practical method for multi-agent path planning in planar domains with obstacles. We used Dynnikov coordinates and revised prioritized planning to efficiently generate homotopically distinct plans. Our experimental results indicate that our method is significantly faster than the method using the Dehornoy order. We also conducted an experiment to optimize the generated plans and compared them with those generated with baseline methods. The results indicated that generating homotopically distinct plans using our method led to an improvement in optimized plans. This showcases the effectiveness of our approach in achieving lower-cost trajectories for multi-agent path planning.

One of the main limitations of our approach is that it cannot consider the homotopical differences that arise only when both sizes of agents and obstacles are taken into account. In scenarios where several agents need to pass through a narrow part where only one agent can pass at a time, homotopy classes of solutions can split, depending on the order in which the agents pass through the narrow section. Figure 19 illustrates such a situation, where the homotopy classes of solutions depend on whether the first agent goes through the narrow section earlier or the second agent does. This phenomenon does not occur when the size of agents can be ignored, as assumed with our approach. There is a computational-geometric difficulty when computing these differences.

Another limitation is the abandonment of optimality. While simple A\* search is workable, it becomes impractical for larger problem instances [Stern, 2019]. To improve efficiency without sacrificing optimality, it may be possible to combine our framework with efficient optimal approaches. To calculate braids while searching, it is required to determine the moves of all agents. This makes it challenging to use conflict-based search, where agent paths are

planned independently in its low-level search. On the other hand, increasing-cost tree search could be a more suitable candidate since it takes into account combinations of all agent paths in its low-level search. Another non-trivial challenge is to make reduction-based methods homotopy-aware.

A potential extension of our research involves exploring decentralized control strategies. Specifically, it may be possible to achieve effective coordination among agents with minimal communication by conveying only braids to other agents.

## A On Presentations of Pure Braid Groups

Bhattacharya and Ghrist [2018] gave a presentation of a homotopy group for path planning with  $n$  agents on a plane, which is a pure braid group  $P_n$ , with the following generators:

$$\{u_{i,j/\gamma_{i+1},\dots,\gamma_{j-1}} \mid 1 \leq i < j \leq n, \gamma_{i+1}, \dots, \gamma_{j-1} \in \{+, -\}\}. \quad (19)$$

The relations are as follows.

- For  $i < j < k$ ,  $\alpha_{i+1}, \dots, \alpha_{j-1} \in \{+, -\}$ , and  $\beta_{j+1}, \dots, \beta_{k-1} \in \{+, -\}$ ,

$$\begin{aligned} & u_{i,j/\alpha_{i+1},\dots,\alpha_{j-1}} \cdot u_{i,k/\alpha_{i+1},\dots,\alpha_{j-1},-\beta_{j+1},\dots,\beta_{k-1}} \cdot u_{j,k/\beta_{j+1},\dots,\beta_{k-1}} \\ & \cdot u_{i,j/\alpha_{i+1},\dots,\alpha_{j-1}}^{-1} \cdot u_{i,k/\alpha_{i+1},\dots,\alpha_{j-1},+\beta_{j+1},\dots,\beta_{k-1}}^{-1} \cdot u_{j,k/\beta_{j+1},\dots,\beta_{k-1}}^{-1}, \end{aligned} \quad (20)$$

$$\begin{aligned} & u_{i,j/\alpha_{i+1},\dots,\alpha_{j-1}} \cdot u_{i,k/\alpha_{i+1},\dots,\alpha_{j-1},-\beta_{j+1},\dots,\beta_{k-1}} \\ & \cdot u_{i,j/\alpha_{i+1},\dots,\alpha_{j-1}}^{-1} \cdot u_{i,k/\alpha_{i+1},\dots,\alpha_{j-1},+\beta_{j+1},\dots,\beta_{k-1}}^{-1}, \end{aligned} \quad (21)$$

and

$$\begin{aligned} & u_{i,k/\alpha_{i+1},\dots,\alpha_{j-1},-\beta_{j+1},\dots,\beta_{k-1}} \cdot u_{j,k/\beta_{j+1},\dots,\beta_{k-1}} \\ & \cdot u_{i,k/\alpha_{i+1},\dots,\alpha_{j-1},+\beta_{j+1},\dots,\beta_{k-1}}^{-1} \cdot u_{j,k/\beta_{j+1},\dots,\beta_{k-1}}^{-1}. \end{aligned} \quad (22)$$

- Let  $i, j, i', j'$  be distinct indices with  $i < j, i' < j', i < i'$ . Let  $\gamma_{i+1}, \dots, \gamma_{j-1} \in \{+, -\}$  and  $\gamma'_{i'+1}, \dots, \gamma'_{j'-1} \in \{+, -\}$  be signs. When  $i < i' < j < j'$ , we assume that  $\gamma_{i'} \neq \gamma'_{i'}$  and  $(\gamma_k, \gamma'_k) \neq (-\gamma_{i'}, \gamma_{i'})$  for all  $i' < k < j$ . When  $i < i' < j' < j$ , we assume that  $\gamma_{i'} = \gamma_{j'}$  and  $(\gamma_k, \gamma'_k) \neq (-\gamma_{i'}, \gamma_{i'})$  for all  $i' < k < j'$ . For such tuples,

$$u_{i,j/\gamma_{i+1},\dots,\gamma_{j-1}} \cdot u_{i',j'/\gamma'_{i'+1},\dots,\gamma'_{j'-1}} \cdot u_{i,j/\gamma_{i+1},\dots,\gamma_{j-1}}^{-1} \cdot u_{i',j'/\gamma'_{i'+1},\dots,\gamma'_{j'-1}}^{-1}. \quad (23)$$

The description in the original paper is incomplete as it omits the condition for the relation (23).

We consider the word

$$w = u_{1,4/-} u_{2,4/-} u_{3,4} u_{1,4/++}^{-1} u_{2,4/+}^{-1} u_{3,4}, \quad (24)$$

which is irreducible when using Dehn's algorithm. On the other hand,

$$\begin{aligned} w &= u_{2,4/-} u_{1,4/+} u_{3,4} u_{1,4/++}^{-1} u_{2,4/+}^{-1} u_{3,4} \\ &= u_{2,4/-} u_{3,4} u_{2,4/+}^{-1} u_{3,4}^{-1} \\ &= u_{3,4} u_{3,4}^{-1} \\ &= e, \end{aligned} \quad (25)$$

where the first, second, and third equalities are deduced from (22) with  $(i, j, k) = (1, 2, 4)$ ,  $(1, 3, 4)$ , and  $(2, 3, 4)$ , respectively. Thus, Dehn's algorithm is incomplete for this presentation when  $n \geq 4$ .

The pure braid group  $P_n$  has a standard presentation [Rolfsen, 2010] using generators  $\{a_{i,j} \mid 1 \leq i < j \leq n\}$  with notation (12) and the following relations.

- For  $1 \leq i < j < k \leq n$ ,

$$a_{i,j} a_{i,k} a_{j,k} a_{i,j}^{-1} a_{j,k}^{-1} a_{i,k}^{-1}, \quad (26)$$

and

$$a_{i,k} a_{j,k} a_{i,j} a_{i,k}^{-1} a_{i,j}^{-1} a_{j,k}^{-1}. \quad (27)$$

- For  $1 \leq i < j < k < l \leq n$ ,

$$a_{i,j} a_{k,l} a_{i,j}^{-1} a_{k,l}^{-1}, \quad (28)$$

$$a_{i,l} a_{j,k} a_{i,l}^{-1} a_{j,k}^{-1}, \quad (29)$$

and

$$a_{i,k} a_{j,l} a_{j,k}^{-1} a_{i,l}^{-1} a_{j,k}^{-1} a_{i,l}^{-1}. \quad (30)$$

Let

$$u_{i,j/\sigma_{i+1},\dots,\sigma_{j-1}} = a_{i,i+1}^{d_{i+1}} \cdots a_{i,j-1}^{d_{j-1}} a_{i,j}^{-d_{j-1}} \cdots a_{i,i+1}^{-d_{i+1}}, \quad (31)$$

where  $d_k = 1$  if  $\sigma_k = +$ , and  $d_k = 0$  if  $\sigma_k = -$ . Then, the relations for  $\{u_{i,j/\sigma_{i+1},\dots,\sigma_{j-1}}\}$  can be deduced from the relations for  $\{a_{i,j}\}$  and vice versa. Therefore, we can translate words from Bhattacharya and Ghrist's presentation to words for the standard presentation. However, this translation increases the lengths of words by a factor of  $O(n)$ . On the other hand, lengths of words constructed by Bhattacharya and Ghrist's method are equal to those of words constructed by the method in § 4.4. To the best of our knowledge, there is no algorithm for the word problem of the pure braid group that is efficient enough to compensate for these drawbacks. This is why we use elements of the braid group to label homotopy classes, instead of those of the pure braid group.

## References

- Aviv Adler, Mark De Berg, Dan Halperin, and Kiril Solovey. Efficient multi-robot motion planning for unlabeled discs in simple polygons. In *Algorithmic Foundations of Robotics XI: Selected Contributions of the Eleventh International Workshop on the Algorithmic Foundations of Robotics*, pages 1–17. Springer, 2015.
- Anton Andreychuk, Konstantin Yakovlev, Pavel Surynek, Dor Atzmon, and Roni Stern. Multi-agent pathfinding with continuous time. *Artificial Intelligence*, page 103662, 2022.
- Felipe Felix Arias, Brian Ichter, Aleksandra Faust, and Nancy M Amato. Avoidance critical probabilistic roadmaps for motion planning in dynamic environments. In *IEEE International Conference on Robotics and Automation*, pages 10264–10270, 2021.
- Emil Artin. Braids and permutations. *Annals of Mathematics*, pages 643–649, 1947a.
- Emil Artin. Theory of braids. *Annals of Mathematics*, pages 101–126, 1947b.
- Roman Barták, Neng-Fa Zhou, Roni Stern, Eli Boyarski, and Pavel Surynek. Modeling and solving the multi-agent pathfinding problem in picat. In *2017 IEEE 29th International Conference on Tools with Artificial Intelligence (ICTAI)*, pages 959–966. IEEE, 2017.
- Sergei Bespamyatnikh. Computing homotopic shortest paths in the plane. *Journal of Algorithms*, 49(2):284–303, 2003.
- Subhrajit Bhattacharya. Search-based path planning with homotopy class constraints. In *Proceedings of the AAAI conference on artificial intelligence*, volume 24, pages 1230–1237, 2010.
- Subhrajit Bhattacharya and Robert Ghrist. Path homotopy invariants and their application to optimal trajectory planning. *Annals of Mathematics and Artificial Intelligence*, 84:139–160, 2018.
- Subhrajit Bhattacharya, Maxim Likhachev, and Vijay Kumar. Identification and representation of homotopy classes of trajectories for search-based path planning in 3d. *Proc. Robot. Sci. Syst.*, pages 9–16, 2011.
- Subhrajit Bhattacharya, Maxim Likhachev, and Vijay Kumar. Topological constraints in search-based robot path planning. *Autonomous Robots*, 33:273–290, 2012.
- Subhrajit Bhattacharya, David Lipsky, Robert Ghrist, and Vijay Kumar. Invariants for homology classes with application to optimal search and planning problem in robotics. *Annals of Mathematics and Artificial Intelligence*, 67(3-4): 251–281, 2013.
- Subhrajit Bhattacharya, Soonkyum Kim, Hordur Heidarsson, Gaurav S Sukhatme, and Vijay Kumar. A topological approach to using cables to separate and manipulate sets of objects. *The International Journal of Robotics Research*, 34(6):799–815, 2015.
- Stephen Bigelow. Braid groups are linear. *Journal of the American Mathematical Society*, 14(2):471–486, 2001.
- Joan Birman, Ki Hyoung Ko, and Sang Jin Lee. A new approach to the word and conjugacy problems in the braid groups. *Advances in Mathematics*, 139(2):322–353, 1998.
- Chao Cao, Peter Trautman, and Soshi Iba. Dynamic channel: A planning framework for crowd navigation. In *2019 international conference on robotics and automation (ICRA)*, pages 5551–5557. IEEE, 2019.

- Michal Čáp, Peter Novák, Alexander Kleiner, and Martin Selecký. Prioritized planning algorithms for trajectory coordination of multiple mobile robots. *IEEE transactions on automation science and engineering*, 12(3):835–849, 2015.
- Michal Čáp, Jean Gregoire, and Emilio Frazzoli. Provably safe and deadlock-free execution of multi-robot plans under delaying disturbances. In *2016 IEEE/RSJ International Conference on Intelligent Robots and Systems (IROS)*, pages 5113–5118. IEEE, 2016.
- Patrick Dehornoy. Braid groups and left distributive operations. *Transactions of the American Mathematical Society*, 345(1):115–150, 1994.
- Patrick Dehornoy. A fast method for comparing braids. *Advances in Mathematics*, 125(2):200–235, 1997.
- Patrick Dehornoy. Efficient solutions to the braid isotopy problem. *Discrete Applied Mathematics*, 156(16):3091–3112, 2008.
- Patrick Dehornoy, Ivan Dynnikov, Dale Rolfsen, and Bert Wiest. Ordering braids. *Mathematical Surveys and Monographs*, 148, 2008.
- Yancy Diaz-Mercado and Magnus Egerstedt. Multirobot mixing via braid groups. *IEEE Transactions on Robotics*, 33(6):1375–1385, 2017.
- Kurt Dresner and Peter Stone. A multiagent approach to autonomous intersection management. *Journal of Artificial Intelligence Research*, 31:591–656, 2008.
- Ivan Alekseevich Dynnikov. On a yang-baxter map and the dehornoy ordering. *Russian Mathematical Surveys*, 57(3):592, 2002.
- Alon Efrat, Stephen G Kobourov, and Anna Lubiw. Computing homotopic shortest paths efficiently. *Computational Geometry*, 35(3):162–172, 2006.
- David BA Epstein. *Word processing in groups*. CRC Press, 1992.
- Michael Erdmann and Tomas Lozano-Perez. On multiple moving objects. *Algorithmica*, 2(1):477–521, 1987.
- Edward Fadell and Lee Neuwirth. Configuration spaces. *Mathematica Scandinavica*, 10:111–118, 1962.
- Ralph Fox and Lee Neuwirth. The braid groups. *Mathematica Scandinavica*, 10:119–126, 1962.
- David Garber, Shmuel Kaplan, and Mina Teicher. A new algorithm for solving the word problem in braid groups. *Advances in Mathematics*, 167(1):142–159, 2002.
- Frank A Garside. The braid group and other groups. *The Quarterly Journal of Mathematics*, 20(1):235–254, 1969.
- Robert Ghrist. Configuration spaces and braid groups on graphs in robotics. *arXiv preprint math/9905023*, 1999.
- Vijay Govindarajan, Subhrajit Bhattacharya, and Vijay Kumar. Human-robot collaborative topological exploration for search and rescue applications. In *Distributed Autonomous Robotic Systems: The 12th International Symposium*, pages 17–32. Springer, 2016.
- Jean Gregoire, Silvère Bonnabel, and Arnaud de La Fortelle. Robust multirobot coordination using priority encoded homotopic constraints. *arXiv preprint arXiv:1306.0785*, 2013.
- Dima Grigoriev and Anatol Slissenko. Computing minimum-link path in a homotopy class amidst semi-algebraic obstacles in the plane. In *Applied Algebra, Algebraic Algorithms and Error-Correcting Codes: 12th International Symposium, AAECC-12 Toulouse, France, June 23–27, 1997 Proceedings 12*, pages 114–129. Springer, 1997.
- Dima Grigoriev and Anatol Slissenko. Polytime algorithm for the shortest path in a homotopy class amidst semi-algebraic obstacles in the plane. In *Proceedings of the 1998 international symposium on Symbolic and algebraic computation*, pages 17–24, 1998.
- Toby Hall and S Öykü Yurttaş. On the topological entropy of families of braids. *Topology and its Applications*, 156(8):1554–1564, 2009.
- Hessam Hamidi-Tehrani. On complexity of the word problem in braid groups and mapping class groups. *Topology and its Applications*, 105(3):237–259, 2000.
- Allen Hatcher. *Algebraic Topology*. Cambridge University Press, 2002.
- Christian Henkel and Marc Toussaint. Optimized directed roadmap graph for multi-agent path finding using stochastic gradient descent. In *Annual ACM Symposium on Applied Computing*, pages 776–783, 2020.
- Emili Hernandez, Marc Carreras, and Pere Ridao. A comparison of homotopic path planning algorithms for robotic applications. *Robotics and Autonomous Systems*, 64:44–58, 2015.

- Wolfgang Hönig, James A Preiss, TK Satish Kumar, Gaurav S Sukhatme, and Nora Ayanian. Trajectory planning for quadrotor swarms. *IEEE Transactions on Robotics*, 34(4):856–869, 2018.
- Kevin D Jenkins. The shortest path problem in the plane with obstacles: A graph modeling approach to producing finite search lists of homotopy classes. Technical report, NAVAL POSTGRADUATE SCHOOL MONTEREY CA, 1991.
- Kazumi Kasaura, Ryo Yonetani, and Mai Nishimura. Periodic multi-agent path planning. *Proceedings of the AAAI Conference on Artificial Intelligence*, 37(5):6183–6191, Jun. 2023. doi: 10.1609/aaai.v37i5.25762. URL <https://ojs.aaai.org/index.php/AAAI/article/view/25762>.
- Michael Khayyat, Alessandro Zanardi, Stefano Arrigoni, and Francesco Braghin. Tactical game-theoretic decision-making with homotopy class constraints. *arXiv preprint arXiv:2406.13656*, 2024.
- Soonkyum Kim, Subhrajit Bhattacharya, and Vijay Kumar. Path planning for a tethered mobile robot. In *2014 IEEE International Conference on Robotics and Automation (ICRA)*, pages 1132–1139. IEEE, 2014.
- Stephen Kloder and Seth Hutchinson. Path planning for permutation-invariant multirobot formations. *IEEE Transactions on Robotics*, 22(4):650–665, 2006.
- Ben Knudsen. Configuration spaces in algebraic topology. *arXiv preprint arXiv:1803.11165*, 2018.
- Donald E Knuth. *The art of computer programming: Volume 3: Sorting and Searching*. Addison-Wesley Professional, 1998.
- Daan Krammer. Braid groups are linear. *Annals of Mathematics*, pages 131–156, 2002.
- Markus Kuderer, Christoph Sprunk, Henrik Kretzschmar, and Wolfram Burgard. Online generation of homotopically distinct navigation paths. In *2014 IEEE International Conference on Robotics and Automation (ICRA)*, pages 6462–6467. IEEE, 2014.
- Rainer Kümmerle, Giorgio Grisetti, Hauke Strasdat, Kurt Konolige, and Wolfram Burgard. g 2 o: A general framework for graph optimization. In *2011 IEEE International Conference on Robotics and Automation*, pages 3607–3613. IEEE, 2011.
- Vitaliy Kurlin. Computing braid groups of graphs with applications to robot motion planning. *Homology, Homotopy and Applications*, 14(1):159–180, 2012.
- Erwin Lejeune, Sampreet Sarkar, and Loig Jezequel. A survey of the multi-agent pathfinding problem. Technical report, Technical Report, Accessed July, 2021.
- Kenneth Levenberg. A method for the solution of certain non-linear problems in least squares. *Quarterly of Applied Mathematics*, 2(2):164–168, 1944.
- Jiaoyang Li, Andrew Tinka, Scott Kiesel, Joseph W Durham, TK Satish Kumar, and Sven Koenig. Lifelong multi-agent path finding in large-scale warehouses. In *International Conference on Autonomous Agents and Multiagent Systems*, pages 1898–1900, 2020.
- Jenny Lin and James McCann. An artin braid group representation of knitting machine state with applications to validation and optimization of fabrication plans. In *2021 IEEE International Conference on Robotics and Automation (ICRA)*, pages 1147–1153. IEEE, 2021.
- Jinyuan Liu, Minglei Fu, Andong Liu, Wenan Zhang, Bo Chen, Ryhor Prakapovich, and Uladzislau Sychou. Homotopy path class encoder based on convex dissection topology. *arXiv preprint arXiv:2302.13026*, 2023.
- Roger C Lyndon, Paul E Schupp, RC Lyndon, and PE Schupp. *Combinatorial group theory*, volume 188. Springer, 1977.
- AV Malyutin. Fast algorithms for identification and comparison of braids. *Journal of Mathematical Sciences*, 119: 101–111, 2004.
- Donald W Marquardt. An algorithm for least-squares estimation of nonlinear parameters. *Journal of the society for Industrial and Applied Mathematics*, 11(2):431–441, 1963.
- Christoforos Mavrogiannis, Jonathan A DeCastro, and Siddhartha Srinivasa. Implicit multiagent coordination at uncontrolled intersections via topological braids. In *International Workshop on the Algorithmic Foundations of Robotics*, pages 368–384. Springer, 2022.
- Christoforos I Mavrogiannis and Ross A Knepper. Multi-agent path topology in support of socially competent navigation planning. *The International Journal of Robotics Research*, 38(2-3):338–356, 2019.
- Christoforos I Mavrogiannis and Ross A Knepper. Multi-agent trajectory prediction and generation with topological invariants enforced by hamiltonian dynamics. In *Algorithmic Foundations of Robotics XIII: Proceedings of the 13th Workshop on the Algorithmic Foundations of Robotics 13*, pages 744–761. Springer, 2020.

- Petr Sergeevich Novikov. On the algorithmic unsolvability of the word problem in group theory. *Trudy Matematicheskogo Instituta imeni VA Steklova*, 44:3–143, 1955.
- Keisuke Okumura, Ryo Yonetani, Mai Nishimura, and Asako Kanezaki. Ctrms: Learning to construct cooperative timed roadmaps for multi-agent path planning in continuous spaces. In *International Joint Conference on Autonomous Agents and Multiagent Systems*, pages 972–981, 2022.
- Junghee Park, Sisir Karumanchi, and Karl Iagnemma. Homotopy-based divide-and-conquer strategy for optimal trajectory planning via mixed-integer programming. *IEEE Transactions on Robotics*, 31(5):1101–1115, 2015.
- David Peifer. An introduction to combinatorial group theory and the word problem. *Mathematics Magazine*, 70(1):3–10, 1997.
- Mike Phillips and Maxim Likhachev. Sipp: Safe interval path planning for dynamic environments. In *IEEE International Conference on Robotics and Automation*, pages 5628–5635, 2011.
- Dale Rolfsen. Tutorial on the braid groups. In *Braids: Introductory Lectures on Braids, Configurations and Their Applications*, pages 1–30. World Scientific, 2010.
- Christoph Rösmann, Frank Hoffmann, and Torsten Bertram. Integrated online trajectory planning and optimization in distinctive topologies. *Robotics and Autonomous Systems*, 88:142–153, 2017.
- Erwin Schmitzberger, Jean-Louis Bouchet, Michel Dufaut, Didier Wolf, and René Husson. Capture of homotopy classes with probabilistic road map. In *IEEE/RSJ International Conference on Intelligent Robots and Systems*, volume 3, pages 2317–2322. IEEE, 2002.
- Guni Sharon, Roni Stern, Meir Goldenberg, and Ariel Felner. The increasing cost tree search for optimal multi-agent pathfinding. *Artificial intelligence*, 195:470–495, 2013.
- Guni Sharon, Roni Stern, Ariel Felner, and Nathan R Sturtevant. Conflict-based search for optimal multi-agent pathfinding. *Artificial Intelligence*, 219:40–66, 2015.
- David Silver. Cooperative pathfinding. In *AAAI Conference on Artificial Intelligence and Interactive Digital Entertainment*, volume 1, pages 117–122, 2005.
- Roni Stern. Multi-agent path finding—an overview. *Artificial Intelligence: 5th RAAI Summer School, Dolgoprudny, Russia, July 4–7, 2019, Tutorial Lectures*, pages 96–115, 2019.
- Roni Stern, Nathan Sturtevant, Ariel Felner, Sven Koenig, Hang Ma, Thayne Walker, Jiaoyang Li, Dor Atzmon, Liron Cohen, TK Kumar, et al. Multi-agent pathfinding: Definitions, variants, and benchmarks. In *Proceedings of the International Symposium on Combinatorial Search*, volume 10, pages 151–158, 2019.
- Pavel Surynek. Multi-agent path finding with continuous time viewed through satisfiability modulo theories (smt). *arXiv preprint arXiv:1903.09820*, 2019.
- Pavel Surynek, Ariel Felner, Roni Stern, and Eli Boyarski. Efficient sat approach to multi-agent path finding under the sum of costs objective. In *Proceedings of the twenty-second european conference on artificial intelligence*, pages 810–818, 2016.
- Jean-Luc Thiffeault. *Braids and Dynamics*, volume 9. Springer Nature, 2022.
- Carsten Thomassen. The jordan-schönflies theorem and the classification of surfaces. *The American Mathematical Monthly*, 99(2):116–130, 1992.
- Benjamin Tovar, Fred Cohen, and Steven M LaValle. Sensor beams, obstacles, and possible paths. In *Algorithmic Foundation of Robotics VIII: Selected Contributions of the Eight International Workshop on the Algorithmic Foundations of Robotics*, pages 317–332. Springer, 2010.
- Paul Vernaza, Venkatraman Narayanan, and Maxim Likhachev. Efficiently finding optimal winding-constrained loops in the plane. In *Proceedings of the International Symposium on Combinatorial Search*, volume 3, pages 200–201, 2012.
- Thayne T Walker, Nathan R Sturtevant, and Ariel Felner. Extended increasing cost tree search for non-unit cost domains. In *International Joint Conference on Artificial Intelligence*, pages 534–540, 2018.
- Konstantin Yakovlev and Anton Andreychuk. Any-angle pathfinding for multiple agents based on sipp algorithm. In *Twenty-Seventh International Conference on Automated Planning and Scheduling*, pages 586–593, 2017.
- Tong Yang, Li Huang, Yue Wang, and Rong Xiong. Efficient search of the k shortest non-homotopic paths by eliminating non-k-optimal topologies. *arXiv preprint arXiv:2207.13604*, 2022.
- Daqing Yi, Michael A Goodrich, and Kevin D Seppi. Homotopy-aware rrt: Toward human-robot topological path-planning. In *2016 11th ACM/IEEE International Conference on Human-Robot Interaction (HRI)*, pages 279–286. IEEE, 2016.

- Jingjin Yu and Steven M LaValle. Multi-agent path planning and network flow. In *Algorithmic Foundations of Robotics X: Proceedings of the Tenth Workshop on the Algorithmic Foundations of Robotics*, pages 157–173. Springer, 2013.
- Matt Zucker, Nathan Ratliff, Anca D Dragan, Mihail Pivtoraiko, Matthew Klingensmith, Christopher M Dellin, J Andrew Bagnell, and Siddhartha S Srinivasa. Chomp: Covariant hamiltonian optimization for motion planning. *The International journal of robotics research*, 32(9-10):1164–1193, 2013.